ISSN 1063-7761, Journal of Experimental and Theoretical Physics, 2011, Vol. 113, No. 1, pp. 80–85. © Pleiades Publishing, Inc., 2011.
Original Russian Text © S.A. Dyakov, E.V. Astrova, T.S. Perova, S.G. Tikhodeev, N.A. Gippius, V.Yu. Timoshenko, 2011, published in Zhurnal Eksperimental'noi i Teoreticheskoi Fiziki, 2011, Vol. 140, No. 1, pp. 92–98.

Optical Properties of Grooved Silicon Microstructures: Theory and Experiment

S. A. Dyakov[a,b]*, E. V. Astrova[c], T. S. Perova[b], S. G. Tikhodeev[d], N. A. Gippius[d], and V. Yu. Timoshenko[a]

[a] *Moscow State University, Moscow, 119991 Russia*
* *e-mail: dyakovs@tcd.ie*
[b] *Trinity College Dublin, Dublin 2, Ireland*
[c] *Ioffe Physicotechnical Institute, Russian Academy of Sciences, St. Petersburg, 194021 Russia*
[d] *Prokhorov General Physics Institute, Russian Academy of Sciences, Moscow, 119991 Russia*

Received October 7, 2010

Abstract—The reflection spectra of grooved silicon structures consisting of alternating silicon walls and grooves (air channels) with a period of $a = 4$–6 μm are studied experimentally and theoretically in the mid-IR spectral range (2–25 μm) upon irradiation of samples by normally incident light polarized along and perpendicular to silicon layers. The calculation is performed by the scattering matrix method taking into account Rayleigh scattering losses in a grooved layer by adding imaginary parts to the refractive indices of silicon and air in grooved regions. The experimental and calculated reflection spectra are in good agreement in the entire spectral range studied. The analysis of experimental and calculated spectra gave close values of the effective refractive indices and birefringence of the studied structures in the long-wavelength spectral region. The values calculated in the effective medium model in the long-wavelength approximation ($\lambda \gg a$) gave considerably understated values. The obtained results confirm the efficiency of the scattering matrix method for describing the optical properties of silicon microstructures.

DOI: 10.1134/S1063776111060161

1. INTRODUCTION

Grooved silicon is a periodic one-dimensional structure consisting of deep trenches with vertical walls. Such structures have interesting optical properties. In the long-wavelength spectral region for $\lambda \gg a$, where a is the lattice period, they reveal the properties of a uniaxial crystal with the high anisotropy of the effective refractive index [1, 2]. For IR light with $\lambda \approx a$, the structure is a one-dimensional photonic crystal with broad stop bands [3, 4]. Grooved silicon excited by a 1.06-μm laser exhibits an enhanced Raman scatterin. [5]. While the optical characteristics of groove structures are well described by the effective medium theory (the so-called approximation of the anisotropic form in a system of parallel plates [6]), spectra in the shorter-wavelength region have not been described theoretically so far.

The aim of this paper is to calculate the reflection and transmission spectra of grooved silicon samples at wavelengths of about the period of the structure and larger and compare them with experiments.

2. EXPERIMENT

Grooved silicon structures can be fabricated by different dry and wet etching methods [7–11]. Among these methods, the anisotropic alkali etching of (110) silicon has an advantage because it enables one to fabricate structures with almost vertical walls having the smoothest surface [12]. The ribs of such structures are formed by the (111) crystallographic planes, which are etched approximately 600 times slower than the (110) planes [9].

We studied grooved silicon structures fabricated on n-type (110) oriented Si wafer with a resistivity of 5 Ω cm prepared by anisotropic etching at 70°C in a 44% aqueous solution of potassium hydroxide. The initial Si wafers were polished from two sides and their surfaces were covered by a thermal oxide or a silicon nitride layer. Then, windows for grooves were opened in this layer on the front of the Si wafer by means of photolithography. The length of these windows was 400 μm and their width was 2–4 μm, depending on the period of the structure. Grooves with walls formed by the (111) planes comprised a lattice with a period a equal to 4, 5, and 6 μm for different samples. Table 1 presents the parameters of samples, and Fig. 1a shows the cross section of one of these structures. Figure 1b shows the schematic of a sample cut along and perpendicular to grooves. It is known that the vertical edges of grooves obtained by anisotropic etching of Si(110) are inclined [9]. In addition, the bottoms of grooves in the studied structures are V-shaped with an apex angle of about 120° [13]. However, in our calculations, we neglect these details and assume for simplicity that the grooves are infinitely long in the direction of the y axis and have a rectangular cross section in the xz plane.

The geometry of optical measurements is shown in Fig. 1b. The reflection and transmission spectra of groove structures were measured in polarized light with Digilab FTS-60A and FTS-6000 Fourier spectrometers in the spectral range from 450 to 6000 cm^{-1} with a resolution of 8 cm^{-1} for the $E_{\parallel}$ and $E_{\perp}$ polarizations. The electric field strength corresponding to the $E_{\parallel}$ or $E_{\perp}$ polarization is directed parallel or perpendicular to grooves, respectively. The spectra are recorded at normal incidence of light to a sample surface.

3. CALCULATION

The reflection and transmission spectra of grooved structures were calculated by the scattering matrix method [14] based on the splitting of the structure into horizontal layers, periodic or homogeneous along the horizontal and homogeneous along the vertical, with expansion of the solutions to the Maxwell equations into a Fourier series and sewing together of the solutions in adjacent layers using the boundary Maxwell conditions. When the incident light illuminates the modulated surface of grooved silicon, the structure behaves like a diffraction grating. The incident wave couples at diffracted (propagating) and exponentially decaying waves, and formally an infinite-dimensional scattering matrix should be used, which is truncated down to a finite-dimensional matrix in numerical calculations.

To formulate the scattering matrix method for photonic-crystal layers, we have to determine the incoming and outgoing states in the scattering problem and develop a method for scattering-matrix calculations that transform incoming solutions to outgoing ones. The method is based on expansion into plane waves in a plane perpendicular to the z axis, and in practice only a finite number N_g of Bragg harmonics are taken into account. In the general case, a two-dimensional diffraction grating couples the incoming light of the frequency ω and wavevector $\mathbf{k} = (k_x, k_y, k_z)$,

$$k_x = \frac{\omega}{c}\sin\vartheta\cos\varphi,$$
$$k_y = \frac{\omega}{c}\sin\vartheta\sin\varphi, \quad (1)$$
$$k_z = \frac{\omega}{c}\cos\vartheta,$$

with all Bragg harmonics at the same frequency ω and wavevectors

$$\mathbf{k}^{\pm}_{\mathbf{G},a} = (k_{x,\mathbf{G}}, k_{y,\mathbf{G}}, \pm k_{z,\mathbf{G},a}). \quad (2)$$

In formulas (1) and (2), ϑ is the angle between vector k and the positive direction of the z axis; φ is the angle between the projection of k onto the xy plane and the x axis,

$$k_{x,\mathbf{G}} = k_x + G_x, \quad k_{y,\mathbf{G}} = k_y + G_y,$$
$$k_{z,\mathbf{G},a} = \sqrt{\frac{\omega^2\varepsilon_a}{c^2} - (k_x + G_x)^2 - (k_y + G_y)^2}, \quad (3)$$

ε_a is the permittivity of vacuum ($a = v$) and on the substrate ($a = s$), and

$$\mathbf{G} = \frac{2\pi}{d}(g_x, g_y, 0), \quad g_{x,y} = 0, \pm1, \pm2, \dots \quad (4)$$

are the vectors of a two-dimensional reciprocal lattice.

The incoming and outgoing sets of the scattering problem are chosen in the form of $4N_g$-dimensional hypervectors $\vec{\mathbb{B}}_{\text{in}}$ and $\vec{\mathbb{B}}_{\text{out}}$ of the composed of the amplitudes of incoming and outgoing plane waves:

$$\vec{\mathbb{B}}_{\text{in}} = \begin{pmatrix} \vec{\mathcal{A}}^{+}_{v} \\ \vec{\mathcal{A}}^{-}_{s} \end{pmatrix}, \quad \vec{\mathbb{B}}_{\text{out}} = \begin{pmatrix} \vec{\mathcal{A}}^{+}_{s} \\ \vec{\mathcal{A}}^{-}_{v} \end{pmatrix}, \quad (5)$$

where $\vec{\mathcal{A}}^{\pm}_{v,s}$ are the $2N_g$-dimensional vectors of partial amplitude of incoming and outgoing plane waves. The full description of the linear optical response of a photonic-crystal layer at the frequency ω can be obtained by calculating the full scattering matrix $\mathbb{S}$ of the system, which connects the incoming vector of amplitudes with the outgoing one:

$$\vec{\mathbb{B}}_{\text{out}} = \mathbb{S}\vec{\mathbb{B}}_{\text{in}}. \quad (6)$$

The full scattering matrix a $(4N_g \times 4N_g)$-dimensional matrix in our case. The calculation of the scattering matrix $\mathbb{S}$ of the photonic-crystal layer involves the following steps:

(i) A photonic-crystal layer is split into a system of layers homogeneous along the z axis (in the case of the model structure in Fig. 2a, these are four layers: a vacuum, a modulated silicon layer, a homogeneous silicon layer, and a vacuum substrate). In each layer, the eigenmodes of the z axis propagation operator are found from the Maxwell equations.

Table 1. Geometrical parameters of slot silicon samples

Sample	Spacing a, μm	Wall thickness d_{Si}, μm	Groove depth l, μm	Total sample thickness H, μm
24a4	4	1.0	30	200
24a5	5	1.2	30	200
24a6	6	1.4	30	200
s5	5	1.8	42	225
s6	6	2.6	42	225

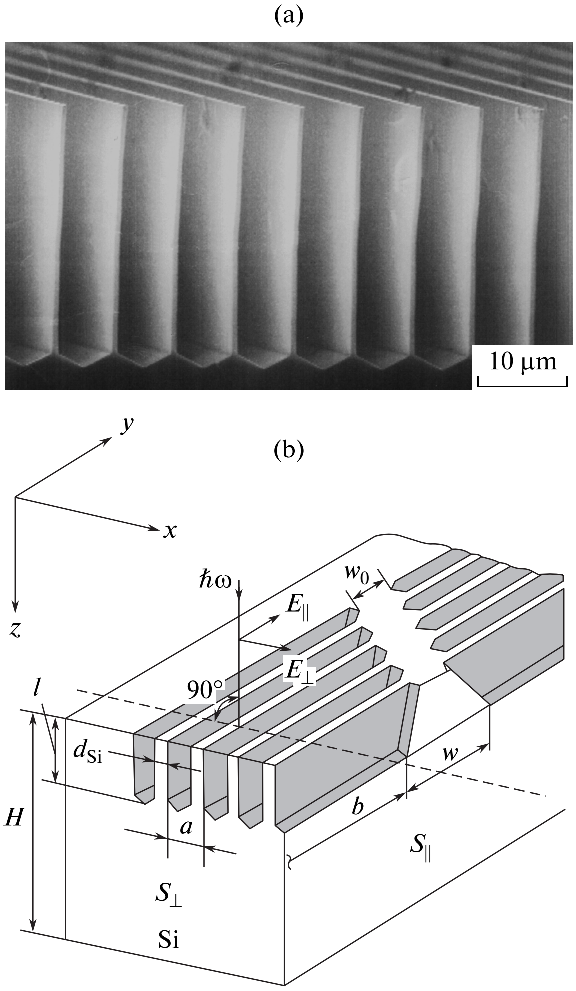

Fig. 1. Structures of grooved silicon: (a) scanning electron microscope image; (b) schematic of the sample and optical measurement: (Si) silicon substrate; $S_\parallel$ ($S_\perp$) section parallel (perpendicular) to grooves; the dashed straight line is the normal to the silicon wall; b is the width of the grooves in the bottom part of the structure; w and w_0 are the widths of solid silicon strips between the grooves on the surface of the sample and the groove depth, respectively.

(ii) The eigenvalues of the propagation operator determine the propagation matrix, while the eigenvectors form the material matrix relating the eigenmode amplitudes of the z axis propagation operator in a layer and the local components of the electromagnetic field.

(iii) Material matrices in two adjacent layers can be used to construct the interface matrix relating eigenmode amplitudes in adjacent layers, and then, by applying the iteration procedure to this matrix (see, for example, [15]), we can calculate the total scattering matrix $\mathbb{S}$ of the whole photonic-crystal structure.

(iv) Knowledge of the components of the scattering matrix allows us to calculate the reflection, transmission, absorption, and diffraction coefficients, and the distribution of electromagnetic fields in the photonic-crystal layer.

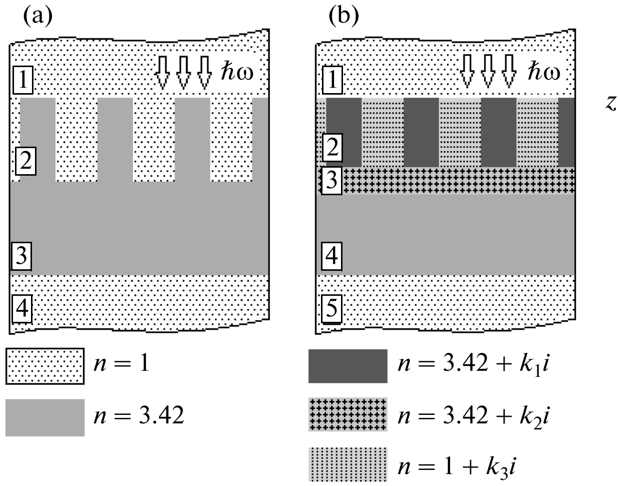

Fig. 2. Schematics of a grooved Si structure for calculations by the scattering matrix method: (a) ideal sample model; (b) real sample model taking diffuse scattering into account.

4. RESULTS AND DISCUSSION

As follows from the above consideration, to calculate the optical properties of a structure, it is necessary to represent it in the form of a sequence of layers homogeneous along the z axis and, possibly, periodic in the direction perpendicular to the z axis. Figure 2a shows an example of sample splitting into layers. The structure is divided into four layers, two of which, the first and the fourth (vacuum), are semi-infinite. The second (silicon/air grooved layer) is periodic in the substrate plane and homogeneous along the z axis, while the third layer (silicon substrate) is completely homogeneous. We selected optical coefficients by neglecting the absorption of light by free carriers in silicon and the interaction of light with crystal lattice phonons.

The reflection spectra calculated for the described model structure considerably differ from the experimental spectra (Fig. 3). The frequent oscillations of the calculated curve (thin grey curve) are related to Fabry–Pérot resonances on a rather thick silicon substrate (~200 μm). To observe them in experiments, the coherence length of light should exceed at least the sample thickness, which is not fulfilled in our case. To exclude such oscillations in calculations, a substrate is usually assumed semi-infinite. The corresponding calculated curve is also shown in Fig. 3 (thin black curve). Now the characteristic frequency of the remaining oscillations of the calculated spectrum approximately corresponds to experiment (they are related to Fabry–Pérot resonances on a grooved silicon layer, see the discussion below); however, the amplitude of these oscillations and the qualitative shape of the spectrum still differ considerably from experimental data.

This discrepancy can be explained by Rayleigh light scattering by the irregularities of the groove struc-

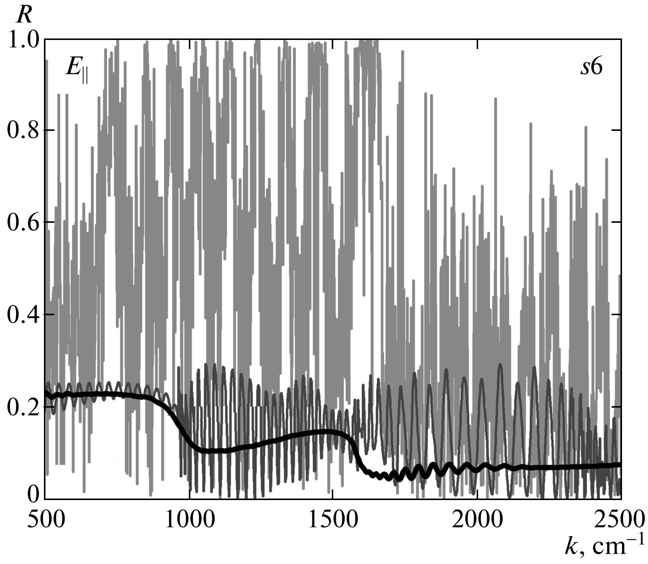

Fig. 3. Experimental (thick curve) reflection spectrum of grooved silicon sample $s6$ and reflection spectra calculated in the ideal sample model for the cases of a finite (Fig. 2a) and semi-infinite silicon substrates (thin grey and black curves, respectively) for the $E_{||}$ polarization of light.

ture both in the modulated layer and the intermediate "modulated part—substrate" layer consisting of V-shaped deepenings in the bottoms of the grooves. Such scattering can be quite considerable because the ratio of the refractive indices of these layers is rather high.

It is well known that the surface roughness introduces considerable errors in the determination of refractive indices of materials by ellipsometry methods [16], especially of their imaginary parts. The latter is quite natural because roughnesses cause a diffuse scattering resulting in losses during the light propagation. There are many examples in the literature (see, for example [17–20]) when scattering losses on the roughness of interfaces were correctly taken into account by adding the imaginary part to real refractive indices of transparent materials or by increasing the imaginary part of the refractive indices of absorbing materials.[1] Following this approach, we will assign complex refractive indices k_1 and k_2 to periodic and intermediate layers, respectively, in silicon and k_3 to air in the periodic layer. We assume for simplicity that parameters k_1, k_2, and k_3 are independent of the wavelength of light.

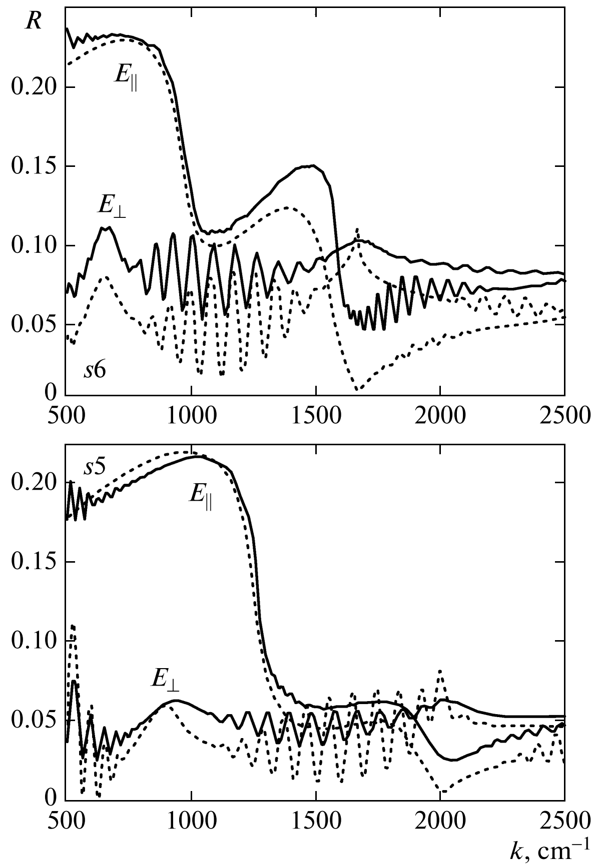

Fig. 4. Experimental (solid curves) and calculated (dashed curves) reflection spectra of grooved silicon samples $s5$ and $s6$ for the $E_{||}$ and $E_\perp$ polarizations. Calculations assume the presence of a scattering layer on the "modulated layer—substrate" interface for which the complex refractive index is set equal to $3.42 + 0.5i$; the refractive index of silicon in the modulated layer is set equal to $3.42 + 0.2i$ and that of air $1 + 0.05i$ (see Fig. 2b).

The resulting model structure is shown in Fig. 2b. The thickness t of the third layer is related to the V-shaped bottom profile and depends on the groove width $t = d_{\text{air}}/2\sqrt{3}$, where $d_{\text{air}} = a - d_{\text{Si}}$ is the groove width.

The numerical simulation shows that parameters k_1 and k_2 begin to make noticeable contributions to reflection spectra at values exceeding 0.1, and k_3 for values above 0.03. Calculations performed with different values of k_1, k_2, and k_3 varied from 0.03 to 3 show that the best fit of experimental reflection spectra is achieved for $k_1 = 0.2$, $k_2 = 0.5$, and $k_3 = 0.05$ (Fig. 4). This procedure provided a good qualitative fit of experimental reflection spectra for other samples as well (Fig. 5).

The obtained experimental and theoretical spectra oscillate due to Fabry–Pérot resonances appearing during the propagation of light through a modulated

[1] Strictly speaking, it is necessary to distinguish the perfectly periodic modulation of interfaces in a photonic-crystal structure and their irregular roughness. Periodic modulations are taken into account in the scattering matrix method and do not require the addition of imaginary parts to take into account radiation losses [14].

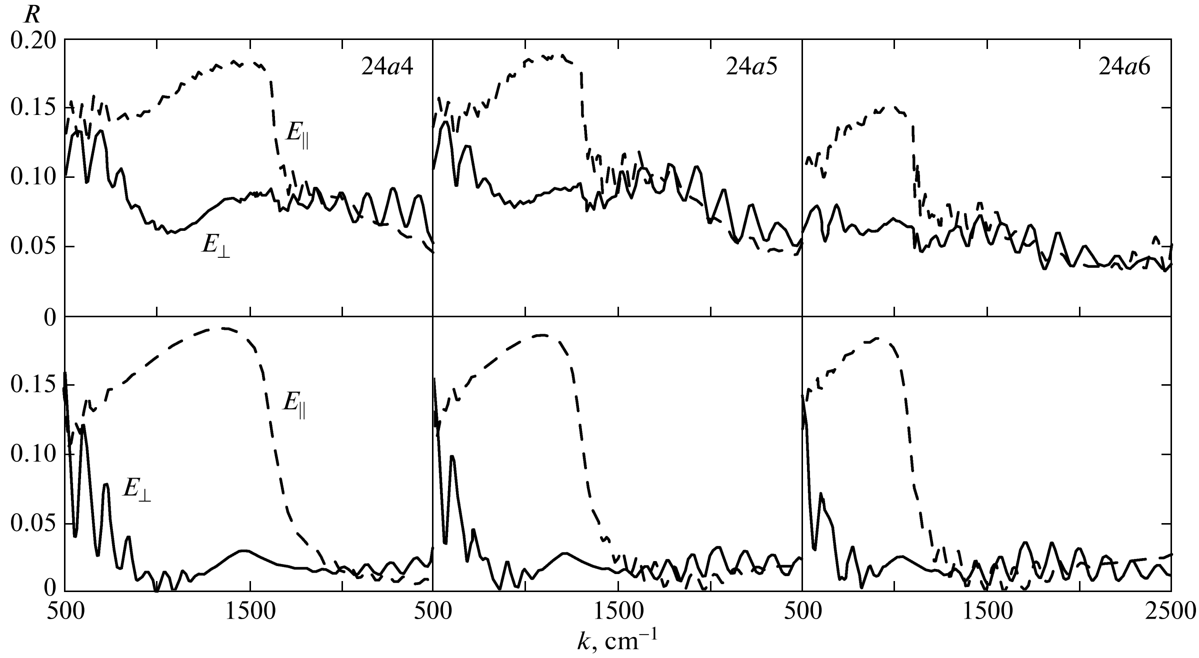

Fig. 5. Experimental (top) and calculated (bottom) reflection spectra of samples 24*a*4, 24*a*5, and 24*a*6.

layer of the structure. By using the Fabry–Pérot resonance condition

$$\Delta\left(\frac{1}{\lambda}\right) = \frac{1}{2n_{\text{eff}}l}, \tag{7}$$

where $\Delta(1/\lambda)$ is the difference of the reciprocal wavelengths of adjacent Fabry–Pérot resonances and l is the grooved layer depth, we can calculate the effective refractive indices n_{eff} of grooved silicon (Table 2) in the low-frequency spectral region, where the effective medium approximation is better fulfilled. These values can be compared with values obtained in the effective medium model for $\lambda \gg a$ [6]:

$$\begin{gathered} n_{\text{eff},\,\|}^2 = f n_{\text{Si}}^2 + (1-f) n_{\text{air}}^2, \\ \frac{1}{n_{\text{eff},\,\perp}^2} = f\frac{1}{n_{\text{Si}}^2} + (1-f)\frac{1}{n_{\text{air}}^2}, \end{gathered} \tag{8}$$

where $n_{\text{eff},\,\|}$ ($n_{\text{eff},\,\perp}$) is the effective refractive index of grooved silicon corresponding to the direction of the electric field wavevector parallel (perpendicular) to the grooves and $f = d_{\text{Si}}/a$ is the filling factor. It follows from Table 2 that the scattering matrix method allows us to calculate the effective refractive indices of periodic silicon layers more accurately than the effective medium theory. For example, the experimental oscillation periods of the reflection coefficient (69 and 125 cm^{-1}) in the low-frequency spectral region for sample 24*a*4 is quite close to these calculated by the scattering matrix method (72 and 127 cm^{-1}). At the same time, the oscillation periods corresponding to Fabry–Pérot resonances in a homogeneous layer with a thickness of l and the refractive indices calculated from expressions (8) are 89 and 148 cm^{-1}. This difference is probably explained by the fact that the condition of applicability of the effective medium approximation $a \ll \lambda$ is not fulfilled accurately enough (in our case, $a/\lambda = 0.18$–0.27).

In the high-frequency region of reflection spectra, the electrostatic approximation condition is not fulfilled ($\lambda \sim a$). The oscillation periods of 140 and 120 cm^{-1} calculated by the scattering matrix method

Table 2. Effective refractive indices of slot silicon calculated from the condition of Fabry–Pérot resonances for experimental reflection spectra and reflection spectra calculated by the scattering matrix method and using the effective medium model

	$n_{\text{eff},\,\|}$			$n_{\text{eff},\,\perp}$			$\Delta n_{\text{eff}} = n_{\text{eff},\,\|} - n_{\text{eff},\,\perp}$		
Sample	24*a*4	24*a*5	24*a*6	24*a*4	24*a*5	24*a*6	24*a*4	24*a*5	24*a*6
Experiment	1.5 ± 0.1	1.7 ± 0.1	1.5 ± 0.1	2.7 ± 0.1	3.0 ± 0.2	3.2 ± 0.3	1.2 ± 0.1	1.2 ± 0.2	1.7 ± 0.3
Scattering matrix method	1.5 ± 0.1	1.7 ± 0.1	1.4 ± 0.2	2.7 ± 0.1	3.0 ± 0.1	3.3 ± 0.2	1.2 ± 0.1	1.3 ± 0.2	1.9 ± 0.3
Effective medium model	1.1 ± 0.1	1.1 ± 0.1	1.1 ± 0.1	1.9 ± 0.1	1.9 ± 0.1	1.9 ± 0.1	0.8 ± 0.1	0.8 ± 0.1	0.8 ± 0.1

in this region are close to their experimental values of 141 and 138 cm^{-1}. The formal use of expressions (7) and (8) gives oscillation periods of 13 and 21 cm^{-1}, which considerably differ from experimental values.

Thus, we have studied the reflection and transmission spectra of grooved silicon structures with different periods and wall thicknesses. The obtained experimental spectra were compared with those calculated by the scattering matrix method. It has been shown that good agreement between experimental data and calculations by the scattering matrix method can be obtained by adding the imaginary parts to the refractive indices of silicon and air in the modulation region to take into account losses caused by Rayleigh scattering of light from the roughness of interfaces.

ACKNOWLEDGMENTS

This work was supported by the Russian Foundation for Basic Research (project nos. 08-02-01408, 09-02-00782). S.A. Dyakov thanks IRCSET (Irish Research Council for Science, Engineering, and Technology) for support.

REFERENCES

1. E. V. Astrova, T. S. Perova, V. A. Tolmachev, A. D. Remenyuk, J. Vij, and A. Moore, Fiz. Tekh. Poluprovodn. (St. Petersburg) **37** (4), 417 (2003) [Semiconductors **37** (4), 399 (2003)].
2. E. Yu. Krutkova, V. Yu. Timoshenko, L. A. Golovan, P. K. Kashkarov, E. V. Astrova, T. S. Perova, B. P. Gorshunov and A. A. Volkov, Fiz. Tekh. Poluprovodn. (St. Petersburg) **40** (7), 855 (2006) [Semiconductors **40** (7), 834 (2006)].
3. V. A. Tolmachev, T. S. Perova, E. V. Astrova, B. Z. Volchek, and J. K. Vij, Phys. Status Solidi A **197** (2), 544 (2003).
4. V. A. Tolmachev, E. V. Astrova, Yu. A. Pilyugina, T. S. Perova, R. A. Moore, and J. K. Vij, Opt. Mater. (Amsterdam) **27** (5), 831 (2005).
5. D. A. Mamichev, V. Yu. Timoshenko, A. V. Zoteyev, L. A. Golovan, E. Yu. Krutkova, A. V. Laktyunkin, P. K. Kashkarov, E. V. Astrova, and T. S. Perova, Phys. Status Solidi B **246** (1), 173 (2009).
6. M. Born and E. Wolf, *Principles of Optics: Electromagnetic Theory of Propagation, Interference, and Diffraction of Light* (Pergamon, London, 1959; Nauka, Moscow, 1973).
7. M. Elwenspoek and H. V. Jansen, *Silicon Micromachining* (Cambridge University Press, Cambridge, 2004).
8. Z. Yu. Gotra, *Technology of Microelectronic Devices: A Handbook* (Radio i Svyaz', Moscow, 1991) [in Russian].
9. D. L. Kendall, Annu. Rev. Mater. Sci. **9**, 373 (1979).
10. G. Barillaro, A. Nannini, and F. Pieri, J. Electrochem. Soc. **149** (3), C180 (2002).
11. E. V. Astrova and G. V. Fedulova, J. Micromech. Microeng. **19**, 095009 (2009).
12. E. V. Astrova, V. A. Tolmachev, Yu. A. Zharova, et al., Solid State Phenom. **156–158**, 547 (2010).
13. A. Holke and H. T. Henderson, J. Micromech. Microeng. **9** (1), 51 (1999).
14. S. G. Tikhodeev, A. L. Yablonskii, E. A. Muljarov, N. A. Gippius, and T. Ishihara, Phys. Rev. B: Condens. Matter **66**, 045102 (2002).
15. D. Y. K. Ko and J. C. Inkson, Phys. Rev. B: Condens. Matter **38**, 9945 (1988).
16. R. M. A. Azzam and N. M. Bashara, *Ellipsometry and Polarized Light* (North-Holland, Amsterdam, The Netherlands, 1987).
17. R. M. A. Azzam and N. M. Bashara, Phys. Rev. B: Solid State **5** (12), 4721 (1973).
18. H. Benisty, D. Labilloy, and C. Weisbuch, Appl. Phys. Lett. **76**, 532 (2000).
19. H. Benisty, Ph. Lalanne, and S. Olivier, Opt. Quantum Electron. **34**, 205 (2002).
20. A. A. Maradudin and D. L. Mills, Phys. Rev. B: Solid State **11**, 1392 (1975).

Translated by M. Sapozhnikov